A nucleostemin-like GTPase required for normal apical and floral meristem development in *Arabidopsis*

Xiaomin Wang, Daniel K. Gingrich, Yunfei Deng, and Zonglie Hong
Department of Plant, Soil, and Entomological Sciences and Program of Microbiology, Molecular Biology and Biochemistry, University of Idaho, Moscow, ID 83844

ABSTRACT **Mammalian nucleostemin (NS) is preferentially expressed in stem cells and acts to promote cell cycle progression. In plants, stem cell activities have to be terminated during flower development, and this process requires the activation of *AGAMOUS* (*AG*) gene expression. Here, a *nucleostemin-like 1* gene, *NSN1*, is shown to be required for flower development in *Arabidopsis*. The *NSN1* mRNA was found in the inflorescence meristem and floral primordia, and its protein was localized to the nucleoli. Both heterozygous and homozygous plants developed defective flowers on inflorescences that were eventually terminated by the formation of carpelloid flowers. Overexpression of *NSN1* resulted in loss of apical dominance and formation of defective flowers. Expression of the *AG* gene was found to be up-regulated in *nsn1*. The carpelloid flower defect of *nsn1* was suppressed by the *ag* mutation in the *nsn1 ag* double mutant, whereas double mutants of *nsn1 apetala2* (*ap2*) displayed enhanced defective floral phenotypes. These results suggest that in the delicately balanced regulatory network, *NSN1* acts to repress *AG* and plays an additive role with *AP2* in floral organ specification. As a midsize nucleolar GTPase, NSN1 represents a new class of regulatory proteins required for flower development in *Arabidopsis*.**

Monitoring Editor
Daniel J. Lew
Duke University

Received: Sep 20, 2011
Revised: Feb 9, 2012
Accepted: Feb 14, 2012

INTRODUCTION

Mammalian nucleostemin (NS) was first discovered in a subtractive screen between embryonic stem cells and differentiated tissue cultures (Tsai and McKay, 2002). It is expressed preferentially in embryonic and adult stem cells, as well as in several cancer cell lines (Tsai and McKay, 2002; Fan *et al.*, 2006; Han *et al.*, 2005). Depletion or overexpression of NS in cultured stem cells impairs cell proliferation, suggesting that it may regulate cell cycle progression (Tsai and McKay, 2002). Targeted deletion of NS in a mutant mouse line results in developmental arrest at the implantation stage, suggesting that NS is required for early embryogenesis (Beekman *et al.*, 2006; Zhu *et al.*, 2006).

Animal NS is a midsize (538 amino acids) GTPase localized to the nucleoli and may shuttle rapidly between the nucleolus and nucleoplasm (Tsai and McKay, 2002, 2005). GTP binding is required for its nucleolar localization, as deletion of the GTP-binding domain of NS results in accumulation of the protein in the nucleoplasm (Tsai and McKay, 2005). One of the major functions of the nucleoli is rRNA transcription and ribosome assembly (Politz *et al.*, 2005). NS is found in the rRNA-free sites within the nucleolar granular component, suggesting that NS serves a function other than ribosome assembly (Politz *et al.*, 2005; Romanova *et al.*, 2009). The unique ability of NS in the regulation of cell cycle progression and stem cell proliferation has been linked both directly and indirectly to p53, MDM2, ribosomal protein RSL1D1, and telomeric repeat–binding factor TRF1 (Beekman *et al.*, 2006; Zhu *et al.*, 2006; Ma and Pederson, 2007; Dai *et al.*, 2008; Jafarnejad *et al.*, 2008). Mammalian NS has also been shown to play a critical role in pre-rRNA processing. Purified NS exists in a large complex that contains three nucleolar proteins involved in pre-rRNA processing (Romanova *et al.*, 2009). Retention of these proteins in the nucleoli is dependent on the presence of NS. The processing of pre-rRNA into 28S rRNA is delayed by the knockdown of NS and promoted by the overexpression of NS. This biochemical evidence demonstrates a role of NS in ribosome

This article was published online ahead of print in MBoC in Press (http://www.molbiolcell.org/cgi/doi/10.1091/mbc.E11-09-0797) on February 22, 2012.

Address correspondence to: Zonglie Hong (zhong@uidaho.edu).

Abbreviations used: *AG*, *AGAMOUS*; *AP*, *APETALA*; *CLV*, *CLAVATA*; NS, nucleostemin; *NSN1*, *nucleostemin-like 1*; TCF, terminal carpelloid flower; *WUS*, *WUSCHEL*.

biogenesis and is consistent with data obtained in yeast and nematode (Du *et al.,* 2006; Kudron and Reinke, 2008). Thus, at the molecular level, NS appears to have multiple biochemical roles.

Pattern formation during flower development has been well studied in the last two decades. Most of the homeotic genes identified so far encode DNA-binding transcription factors. *AGAMOUS* (*AG*), encoding a MADS domain–containing transcription factor, commences to express at the central part of stage 3 flower primordia and is accumulated in whorls 3 and 4 in older floral primordia (Yanofsky *et al.,* 1990; Bowman *et al.,* 1991). *AG* functions to specify the stamen and carpel identities and controls floral meristem determinacy (Mizukami and Ma, 1997; Lohmann *et al.,* 2001; Sun *et al.,* 2009). In *ag-1*, stamens and carpels are replaced by a new flower that only has sepals and petal (Bowman *et al.,* 1989). When *AG* is overexpressed, inflorescence meristem becomes determinate and produces terminal flowers (Mizukami and Ma, 1992, 1997). *HUA1, HUA2, HUA1 ENHANCER 1* (*HEN1*), and *HUA2 ENHANCER2* (*HEN2*) are components of the *AG* pathway. Among them, *HUA2* and *HEN1* play important roles in specifying stamen and carpel identity (Chen and Meyerowitz, 1999; Chen *et al.*, 2002). *APELATA2* (*AP2*), encoding a transcription factor that does not contain a MADS box, acts to specify the identity of whorl 1 and 2 floral organs (Jofuku *et al.,* 1994). In *ap2* mutants, sepals are transformed into carpelloid structures (Bowman *et al.,* 1991). *AP2* and *AG* reciprocally repress gene expression of each other (Bowman *et al.,* 1991; Drews *et al.,* 1991).

Regulation of *AG* transcription requires sequences located in its 3-kb second intron, which serves as a binding site for positive and negative regulators (Sieburth and Meyerowitz, 1997; Busch *et al.,* 1999). As positive regulators, WUSCHEL (WUS) and LEAFY (LFY) bind to this regulatory intron sequence and activate *AG* gene expression (Lenhard *et al.,* 2001; Lohmann *et al.,* 2001). Negative regulators, including AP2, LEUNIG (LUG), SEU (SEUSS), BELL-RINGER (BLR), and PERIANTHIA (PAN), are also known to regulate *AG* via this intron sequence (Liu and Meyerowitz, 1995; Deyholos and Sieburth, 2000; Franks *et al.,* 2002; Bao *et al.,* 2004; Sridhar *et al.,* 2004; Das *et al.,* 2009).

We were interested in understanding a potential role of NS homologues in plants. In this study, we identified a *nucleostemin-like 1* (*NSN1*) gene in *Arabidopsis* and characterized a knockout mutant of this gene (*nsn1-1*). As a nucleolar GTPase, NSN1 represents a new class of proteins that play a critical role in controlling floral identity and maintenance of inflorescence meristem. At the genetic level, *NSN1* acts as an *AG* repressor and is required for the maintenance of inflorescence meristem identity and flower development in *Arabidopsis*.

RESULTS

A midsize GTPase with homology to animal nucleostemins

In a search for GTP-binding proteins that may play a role in cell division control, we cloned the *Arabidopsis* NSN1 (At3g07050) cDNA. The deduced NSN1 polypeptide, consisting of 582 amino acid residues with calculated molecular mass of 65.8 kDa (Figure 1A), contains multiple functional motifs, including five potential nuclear localization signals, a basic domain, a coiled-coil domain, a GTP-binding region, an RNA-binding domain, and an acidic domain (Figure 1B). The conserved GTP-binding motifs are arranged in a circularly permutated order (G5-G4-G1-G2-G3; Daigle *et al.,* 2002). NSN1 shares 30 and 31% amino acid sequence identity with human NS and GNL3L, respectively, but is less homologous to human NGP1 (25% identity; Supplemental Figure S1). In *Arabidopsis*, the most closely related protein, At1g52980, has only 25% sequence identity with NSN1, suggesting that *NSN1* is a unique gene. At1g52980, referred to as *AtNGP1*, represents an uncharacterized paralogue of *NSN1* in *Arabidopsis*. Both NSN1 and NGP1 proteins belong to a new GTPase family with a signature MMR/HSR1 domain (Daigle *et al.,* 2002). This GTPase family is conserved in organisms ranging from Archaea to vertebrates (Reynaud *et al.,* 2005; Meng *et al.,* 2007) and can be grouped into at least four subfamilies (Figure 1C). The human and mouse genomes contain three members for each genome—*NS*, *GNL3L*, and *NGP1*—whereas *Arabidopsis* and rice have two members—*NSN1* and *NGP1*—per genome. *Dictyostelium*, on the other hand, has only one *NSN1* member.

Loss-of-function mutants

To investigate the function of *NSN1*, we characterized two *Arabidopsis* mutants *nsn1-1* and *nsn1-2*, the former having T-DNA inserted in the eighth intron and the latter containing a transposon in the second exon (Figure 2A). The two mutant lines had indistinguishable growth and reproduction phenotypes (Supplemental Figure S2), suggesting that the defects observed are caused by mutations of the same locus, At3g07050. Further molecular characterization was conducted in *nsn1-1* unless indicated otherwise. T-DNA insertion in the *NSN1* gene was confirmed by genomic PCR (Supplemental Figure S3), and the knockout of *NSN1* gene expression in homozygous lines was verified by reverse transcriptase (RT)-PCR (Figure 1B). This analysis suggests that *nsn1-1* is a null mutation. The mutant exhibited pleiotropic defects in growth and development, with the most striking phenotypes in the formation of defective flowers and siliques (see later discussion).

Termination of inflorescence meristem and homeotic floral organ transformation

We characterized both heterozygous (*nsn1/+*) and homozygous *nsn1* plants because they showed different degrees of defects in seedling growth and reproductive fertility. Both heterozygous and homozygous plants had highly reduced self-fertility, and the latter phenotype was much more severe (Figure 2C and Supplemental Figure S2C). Heterozygous *nsn1*/+ plants were comparable to the wild type in vegetative growth but developed defective flowers and produced short siliques. The main and branch inflorescence meristems in *nsn1*/+ were also characteristically transformed into determinate apexes by developing a terminal carpelloid flower on each apex. A typical terminal carpelloid flower of *nsn1*/+ exhibited a complete absence of petals in whorl 2 and contained a reduced number of deformed stamens in whorl 3 (Figure 2, G and H). Both heterozygous and homozygous *nsn1* plants produced carpelloid flowers that were characterized by the homeotic transformation of sepals in whorl 1 into carpelloid sepals (Figure 2, H and I). Carpelloid flowers were also produced at various flower positions of the upper inflorescences of *nsn1-1* plants (Supplemental Figure S5). The pistil of *nsn1*/+ carpelloid flowers morphologically resembled that of the control flowers, except that the two carpels often became dehiscent and contained aberrant ovule-like and stamen-like structures inside the locule. Homozygous *nsn1* plants exhibited much more severe flower defects. The flowers lacked floral organs of whorls 2 and 3 and instead developed stigma-like, style-like, and ovule-like structures (Figure 2I). Homozygous *nsn1* plants also had severe developmental defects in shoot apex (Figure 2F). The transformation of an inflorescence meristem to a terminal floral primordium took place in 40- to 45-d-old *nsn1* plants. In wild-type (WT) plants, the inflorescence meristems stop to develop floral organs when they are ~50 d old (Figure 2, F and G). This supports that NSN1 is required for the

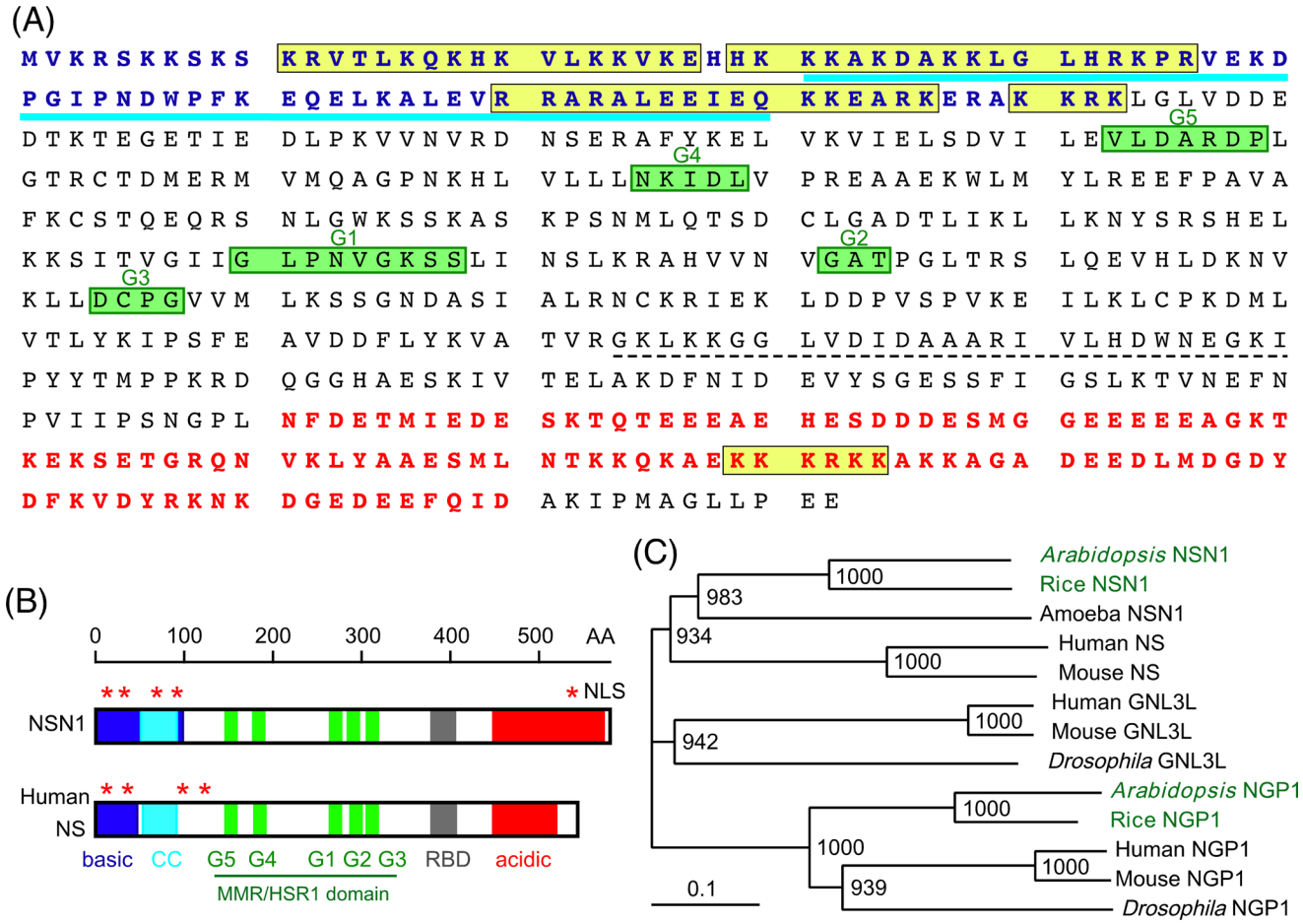

FIGURE 1: Functional motifs and phylogenetic tree of *Arabidopsis nsn1*. (A) Amino acid sequence of NSN1 (At3g07050). Blue, basic domain (basic); blue underline, coiled-coil domain (CC); yellow boxes, nuclear localization signals (NLS); green boxes, GTP-binding motifs (G1–G5); dashed underline, RNA-binding domain (RBD); red, acidic domain (acidic). (B) Comparison of *Arabidopsis* NSN1 with human NS. The GTP-binding motifs (G1–G5) in NSN1 are arranged in a circularly permuted manner known as the MMR/HSR1 domain. Five NLS motifs are indicated by asterisks. Shaded areas correspond to the structural domains indicated in A. (C) Phylogenetic tree of NSN1 homologues. Human and mouse contains three *NS*-related genes (*NS*, *GNL3L*, and *NGP1*), whereas *Arabidopsis* and rice have two (*NSN1* and *NGP1*). The amoeba *Dictyostelium* has only one *NSN1* gene. Peptide sequences used for phylogenetic analysis include At3g07050 (AtNSN1), At1g52980 (AtNGP1), Os01g0375000 (rice NSN1), Os03g0352400 (rice NGP1), AAV74413 (human NS), AAH11720 (human GNL3L), Q13823 (human NGP1), AAO19472 (mouse NS), NP_932778 (mouse GNL3L), NP_663527 (mouse NGP1), Q8MT06 (*Drosophila* NGL3L), EAL25205 (*Drosophila* NGP1), and Q54KS4 (amoeba NSN1). Bootstrap values from 1000 trials are displayed on nodes.

maintenance of inflorescence meristem. Scanning electronic microscopy revealed that the inflorescence meristem dome of *nsn1* was smaller than that of WT plants at young stages (20 d old; Supplemental Figure S6). Taken together, these data suggest that the loss of function of *NSN1* results in an increase in the chance of changing earlier cell fate of inflorescence meristem and floral meristem from indeterminate to determinate.

Complementation of *nsn1*

To confirm that the phenotypes of *nsn1* were caused by a mutation in the *NSN1* locus, we transformed the heterozygous *nsn1-1/+* plants with *JAtY64G16*, a TAC clone containing At3g07050 and 18 other putative genes. After genome typing, T2 plants carrying *JAtY64G16* in the homozygous *nsn1* genomic background were maintained. Their T3 progeny ($NSN1^C$) were scored phenotypically for complementation. Reproductive phenotypes of $NSN1^C$ were significantly different from those of the heterozygote *nsn1* plants (see later discussion) and were fully restored to those of the WT control (Figure 3, A–C). Flower morphology and silique length of $NSN1^C$ were indistinguishable from the WT. In opened siliques of heterozygote *nsn1/+*, there were frequent unfertilized ovules, arrested embryos, and aborted seeds, which were not observed in $NSN1^C$ siliques (Figure 3C). On average, an *nsn1* silique contained only 6.4 ± 3.8 seeds (n = 10 siliques), whereas WT and $NSN1^C$ produced 60.6 ± 1.7 and 64.4 ± 7.9 seeds per silique, respectively. This complementation test demonstrated that 1 of the 19 genes in the *JAtY64G16* TAC clone is responsible for the observed floral and fertility phenotypes. When the complementation result was combined with the observation that two independent mutant alleles of *nsn1* (i.e., *nsn1-1* and *nsn1-2*; see Supplemental Figure S2) exhibited identical growth and reproduction phenotypes, we concluded that the defective phenotypes of *nsn1* plants are caused by the mutation at the *NSN1* locus (At3g07050).

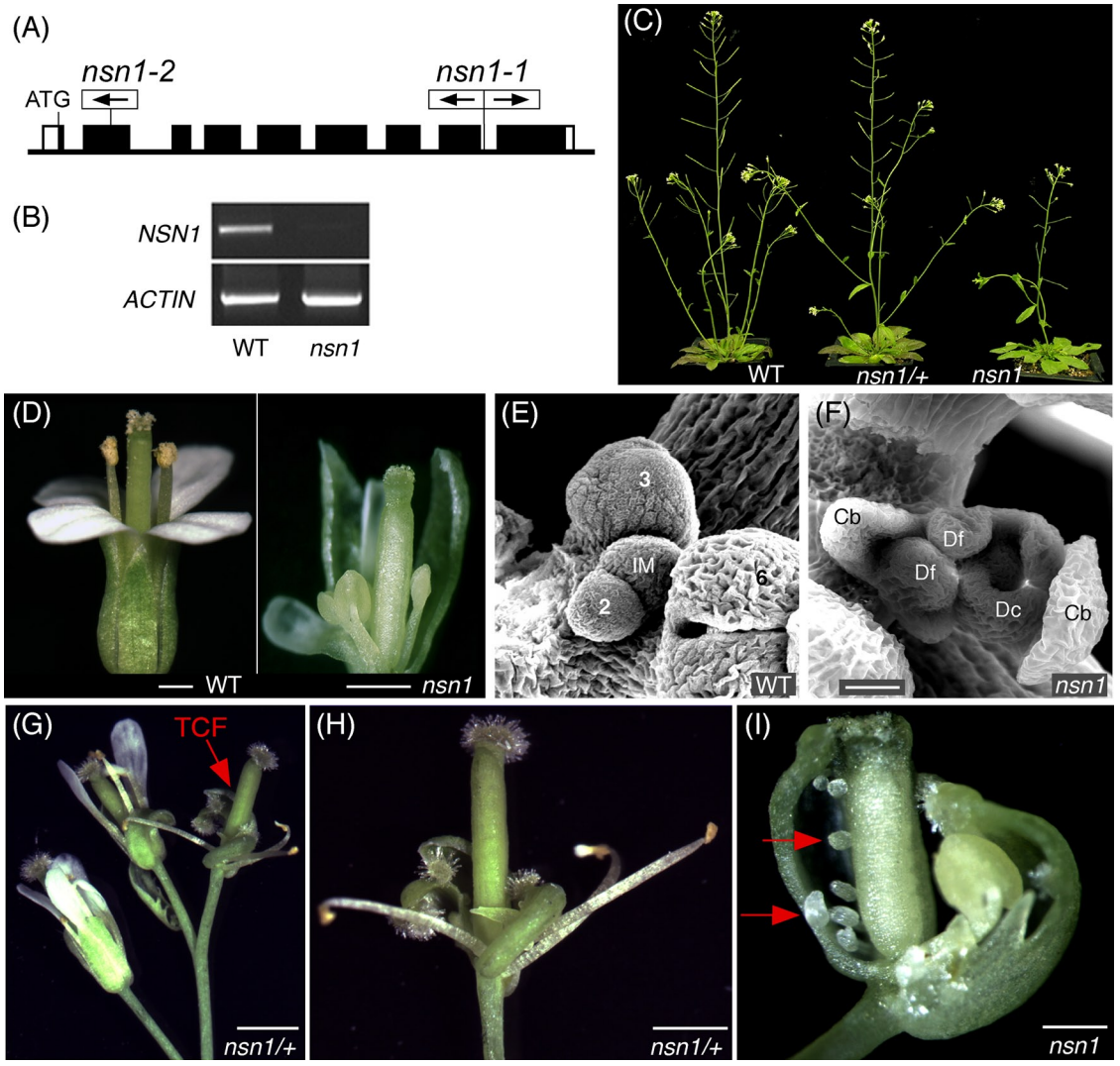

FIGURE 2: Termination of inflorescence meristem and homeotic transformation of floral organs in *nsn1*. (A) *nsn1-1* (SALK_029201) contained two T-DNA inserts in the eighth intron of the *NSN1* gene, and *nsn1-2* (RAFL11-2045-1) had one transposon in the second exon. Framed arrows indicate the direction of T-DNA or transposon. (B) RT-PCR showing the lack of detectable *NSN1* mRNA in homozygous *nsn1-1* plants. *ACTIN* mRNA served as a control. Nsn1-LP and Nsn1-RP were used as primers (for their positions see Supplemental Figure S3A) for RT-PCR, which generated a cDNA fragment of 1050 base pairs. (C) Phenotypes of 30-d-old WT, *nsn1-1/+*, and *nsn1* plants. Heterozygous *nsn1/+* plants showed no obvious growth phenotype but had significant defects in reproduction. Homozygous *nsn1* plants were very small and yielded only a few seeds per plant. (D) A flower at position 25 from the lower part of inflorescence of a 40-d-old *nsn1-1* plant had a reduced number of petals and shortened stamen filaments as compared with a WT flower at the same position of inflorescence. (E, F) Scanning electronic images of the inflorescence meristem (IM) of 40-d-old WT (E) and *nsn1* (F) plants. Note that the inflorescence meristem (F) was terminated by the formation of a terminal carpelloid flower (TCF). Cb, carpelloid bract; Dc, defective carpel; Df, defective floral meristem developed inside a TCF. Stages of the WT floral primordia (E) are indicated. (G–I) Inflorescences of *nsn1/+* and *nsn1* were terminated by the formation of a TCF (red arrow in G), which is shown in a higher magnification (H). A typical TCF of *nsn1* would contain homeotically transformed carpelloid bracts, severely defective stamens, and no petals (I). Ectopically developed ovules are indicated by red arrows (I). Shown are the terminal carpelloid flowers at position 35 of *nsn1-1/+* (H) and position 36 of *nsn1-1* (I). Scale bars, 25 μm (E, F), 2 mm (G), 1 mm (D, H, I).

Localization in the nucleoli

We expressed a green fluorescent protein (GFP)–tagged NSN1 in tobacco BY-2 cells and in transgenic *Arabidopsis* plants. NSN1 was localized to the nucleoli in BY-2 cells (Figure 4C). In transgenic plants, GFP alone was distributed uniformly in the nuclei and cytoplasm (Figure 4H). However, GFP-tagged NSN1 was concentrated in the nucleoli with a lower but detectable level of presence in the nucleoplasm (Figure 4G). It has been shown that the N-terminal lysine-rich domain (KRD) of the animal NS and GNL3L serves as the nucleolar localization signal, whereas the GTP-binding domain is required for efficient retention of the protein in the nucleoli (Meng *et al.*, 2007). It is not known whether the N-terminal KRD of NSN1 is responsible for its nucleolar targeting.

Expression in the inflorescence and floral meristems

We measured the expression of *NSN1* mRNA in different tissues of *Arabidopsis* plants by RT-PCR and found that its expression was highly concentrated in apical meristem and developing flowers and

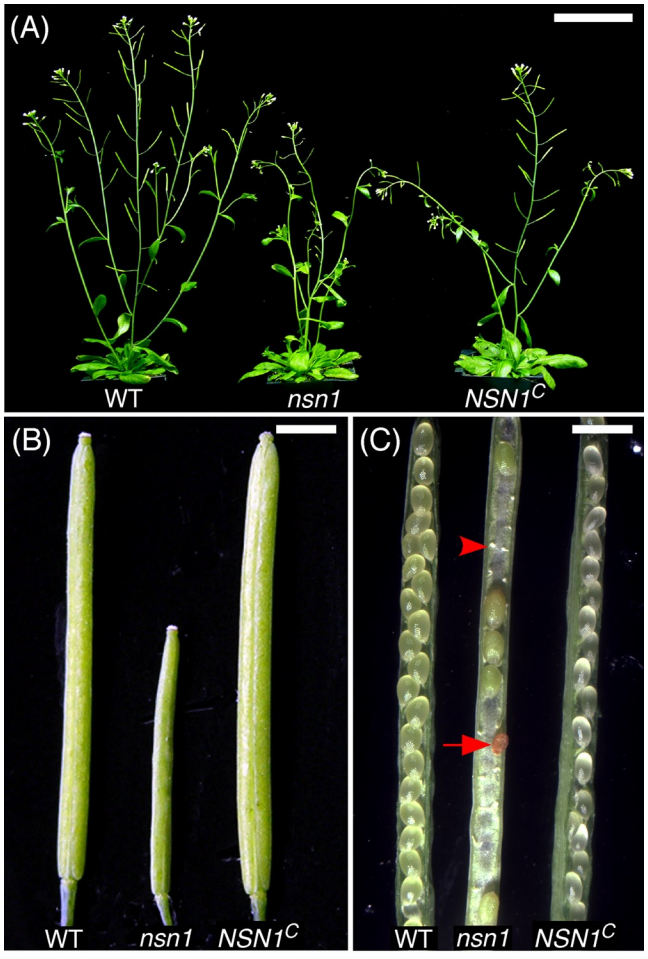

FIGURE 3: Complementation of *nsn1-1* using a genomic DNA fragment containing At3g07050. (A) The 30-d-old adult plants of the wild-type (WT), *nsn1-1*, and the homozygous mutant *nsn1-1* containing At3g07050 (*NSN1*^{C}). The length of siliques was longer in *NSN1*^{C} than in *nsn1* and was comparable to that of the wild type. (B) Siliques were thicker in *NSN1*^{C} plants than in *nsn1-1* and were comparable to that of the wild type. (C) Unfertilized ovules (arrowhead) and aborted embryos (arrow) were present in *nsn1-1* siliques but absent in *NSN1*^{C} and wild type plants, suggesting full complementation in *NSN1*^{C}. Scale bars, 5 cm (A), 6 cm (B, C).

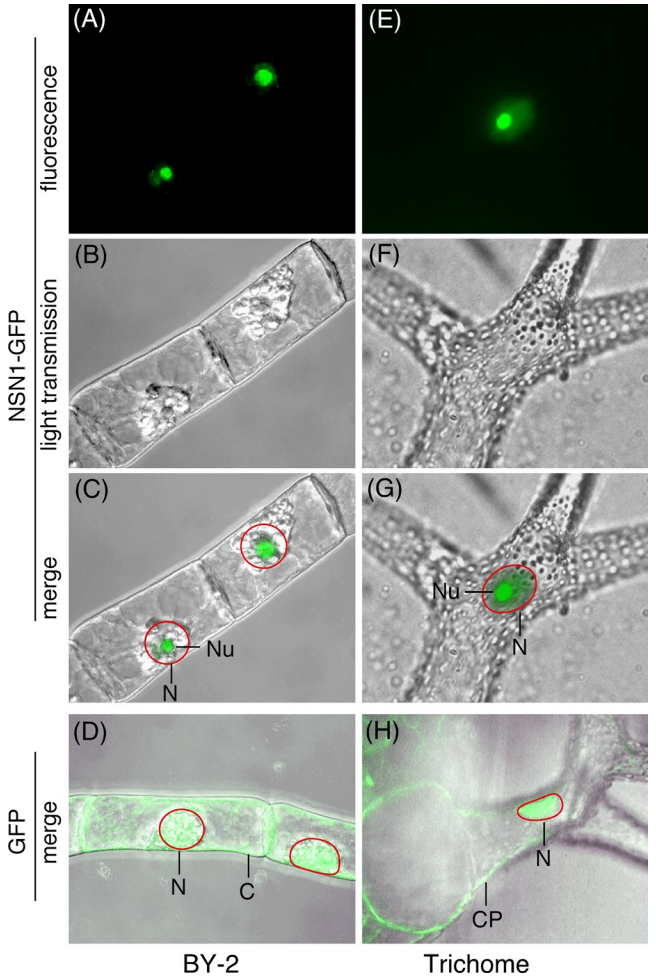

FIGURE 4: Nucleolar localization of NSN1. (A–D) Tobacco BY-2 cells expressing GFP-tagged NSN1 (A–C) or GFP control (D). (E–H) *Arabidopsis* trichomes expressing GFP-tagged NSN1 (E–G) or GFP control (H). Green fluorescence images of cells (A, E) were superimposed with the light transmission views (B, F), generating merged images (C, G). For GFP controls, only the merged images (D, H) are shown. CP, cytoplasm; N, nucleus; Nu, nucleolus. Red circles in C, D, G, and H indicate nuclear boundaries.

siliques, although its mRNA could be detected at relatively low levels in most tissues tested (Supplemental Figure S3D). This expression pattern was consistent with data deposited in the online database GENEVISTIGATOR (www.genevestigator.com), which shows that high expression levels of *NSN1* are detected in inflorescence, flower, seed, and shoot apex (Supplemental Figure S4). We performed in situ RNA hybridization to examine the cellular expression pattern of *NSN1* in inflorescence meristems and developing flowers. The expression of *NSN1* was found to be very low in the inflorescence meristem dome as compared with that in the floral primordia (Figure 5A). Its expression was detectable in floral primordia as early as at stage 1 of floral primordia (Figure 5A). The expression was highly elevated at stages 2 to 3 (Figure 5B). *NSN1* mRNA became concentrated in the primordia of stamens and carpels at stages 5 to 6 (Figure 5C). At the later stages of floral development, *NSN1* was expressed primarily in developing microspores in the stamens and ovules in the carpels (Figure 5, E and F). This expression pattern of *NSN1* is consistent with its putative role in the regulation of floral development.

Ectopic *AG* expression in *nsn1* mutants

The *nsn1* carpelloid flowers were anatomically similar to those developed on the *bellringer* (*blr*) mutant that is defective in a homeobox-containing transcription factor. The BLR protein binds to the promoter of the floral homeotic gene *AG*, repressing its expression (Bao *et al.*, 2004). We reasoned that NSN1 might also exert its effects on floral organ identity through regulation of *AG* gene expression in a yet-to-be-identified manner since NSN1 is not a transcription factor but a nucleolar GTP-binding protein. We examined the expression pattern of *AG* in the *nsn1/+* mutant. In wild type, *AG* is not expressed in the inflorescence meristem at all, nor is it in the floral meristem prior to stage 3 (Sieburth *et al.*, 1995; Lenhard *et al.*, 2001; Lohmann *et al.*, 2001). In *nsn1/+*, *AG* mRNA could be detected in floral primordia of as early as stage 2, as well as in the whole terminal carpelloid floral primordium (Figure 6C). In flowers of stages 3 to 4 of *nsn1/+*, *AG* was expressed not only in the central parts (whorls 3 to 4) of a floral meristem, but also in whorl 1 sepal primordia (Figure 6B), suggesting that *AG* expression may be repressed by *NSN1*.

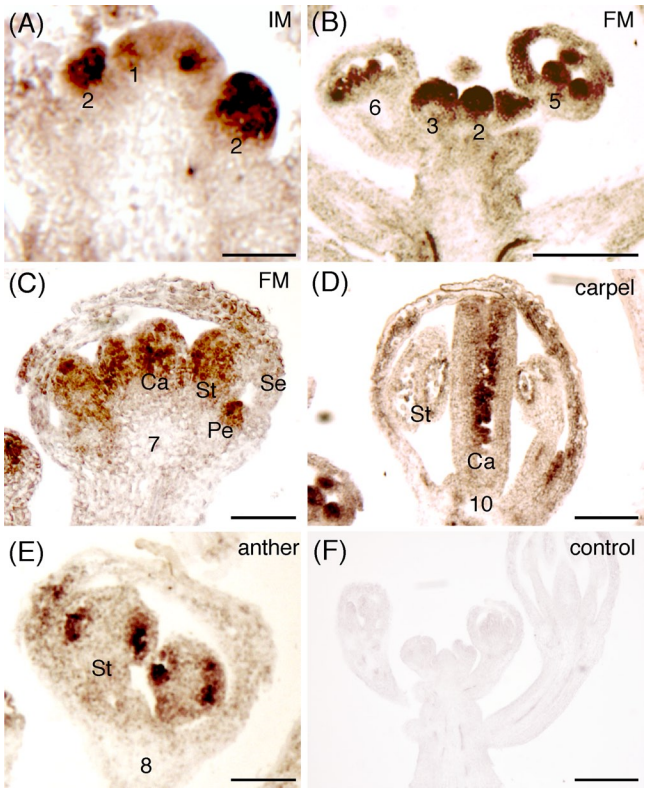

FIGURE 5: In situ hybridization of *NSN1* mRNA in the inflorescence meristem (IM) and floral meristem (FM). (A–E) Sections of *Arabidopsis* IM (A), FM (B, C), carpels (D), and anther (E) probed with the antisense *NSN1* mRNA labeled with digoxigenin. The floral developmental stages are designated by numbers. Note that *NSN1* was expressed at high levels in the stage 2 floral primordia, in the stamens and carpels at stage 6, in pollen grains and ovules at stage 10, and in all four whorls at stage 7. Ca, carpel; Pe, petal; Se, sepal; St, stamen. (F) The control section reacted with the sense *NSN1* mRNA. Scale bars, 25 μm (A, C–E), 100 μm (B, F).

To confirm the *AG* ectopic expression pattern observed by in situ hybridization, we introduced the KB9 construct (*AG::GUS*) into *nsn1* plants. This construct contained the regulatory elements of *AG*, including the 3-kb second intron, and would allow for observing *AG* gene expression by monitoring the activity of the β-glucuronidase (GUS) reporter (Busch *et al.*, 1999; Lohmann *et al.*, 2001). In the control plant harboring KB9, the GUS activity was detected only in the post–stage 3 floral meristems but not in the inflorescence meristem (Figure 6D), which is consistent with the in situ hybridization result. In *nsn1* plants expressing the same construct, GUS staining was drastically enhanced across the regions of inflorescence meristem and floral meristem and floral primordia (Figure 6E). In *nsn1* carpelloid flowers, GUS was expressed in all carpelloid structures, including the ovule-like ones developed on the homeotically transformed carpelloid bracts (Figure 6F). These data suggest that the termination of the inflorescence meristem and the homeotic transformation of floral organs in *nsn1* are caused by *AG* ectopic expression and indicate a pivotal role of *NSN1* as a negative regulator for *AG* expression.

Suppression of the terminal carpelloid flower defects of *NSN1* by *AG* mutation

To examine the genetic relationship between *NSN1* and *AG*, we generated *nsn1-1 ag* double mutation plants by crossing *nsn1/+* (Columbia-0) into *ag/+* (Landsberg). Seven F1 plants were confirmed to contain the *nsn1* mutation using genomic PCR (unpublished data). These plants also exhibited the characteristic *ag/+* silique phenotype with three carpels in one silique. From the segregated F2 individuals, *nsn1-1 ag* double mutant was identified on the basis of genomic PCR and flower phenotype of *ag* mutant. The double-mutant plants phenocopied *ag* mutation and produced flowers with multiple layers of sepals and petals with no staminoid and carpelloid tissues (Figure 6I). This was in contrast to the carpelloid flowers of *nsn1-1*, which typically contained carpelloid bracts at whorl 1 and a reduced number of petals and stamens (Figure 6G). The size of *nsn1-1 ag* double-mutant flowers was smaller than those of *ag* (Figure 6H), which was likely to have resulted from the difference in the ecotype background. This result suggests that the terminal carpelloid flower phenotype of *nsn1* depends on the activity of *AG* and may be caused by expanded ectopic *AG* expression in the *nsn1* floral meristem. These findings support the hypothesis that NSN1 may act as an upstream regulator of *AG*.

Genetic enhancement of *ap2* phenotypes by *nsn1*

To analyze whether the ectopic *AG* expression during floral development in *nsn1* was dependent upon *APETALA2* (*AP2*), we introduced two *ap2* loss-of-function mutations (*ap2-1* and *ap2-2*) into the *nsn1-1* mutant. In flowers of *ap2-1*, a weak *ap2* allele, organs of whorls 1 and 2 were converted into leafy bracts (4.0 ± 0) and staminoid petals (4.0 ± 0), respectively, whereas the stamens (6.0 ± 0) and carpels (2.0 ± 0) remained normal in whorls 3 and 4 (Figure 7A). Flowers of *nsn1-1 ap2-1* double mutants were more severely defective than those of either of the single mutant (Supplemental Table S1). The number of whorl 1 organs was reduced from 4.0 ± 0 to 3.4 ± 0.9, and they included leafy bracts in lateral positions and carpelloid bracts in medial positions (Figure 7B and Supplemental Table S1). In addition, whorl 2 organs disappeared completely. This phenotype of the double mutant was more severe than that of *ap2-1* single mutant and very close to that of *ap2-2*, a strong mutant allele. In *ap2-2*, the four whorl 1 organs were converted into two medial carpel and two lateral leafy bracts. There were no organs in whorls 2 and 3, whereas whorl 4 contained normal carpels (Figure 7C). In *nsn1-1 ap2-2* double mutant, the whorl 1 organs were converted into a carpelloid cylinder that partially or completely surrounded a normal whorl 4 gynoecium (Figure 7, D and E, and Supplemental Table S1). Stigmatic tissue was developed on the edge of the carpelloid cylinder, and ovules and degenerated stamens were present on the interior wall of the cylinder (Figure 7D). Some double-mutant flowers became an open gynoecium consisting of two medial carpel and numerous carpelloid filaments with stigmatic tissue on their tips (Figure 7F). Thus the homeotic transformation was enhanced in *nsn1 ap2-2* double mutant as compared with that of either single mutant. The additive effect of *AP2* and *NSN1* on flower formation suggests that the two genes have distinct roles in floral development, possibly via independent repression of the *AG* gene.

Deleterious growth and reproductive defects caused by *NSN1* overexpression

After several transformation attempts, we obtained a total of six transgenic plants expressing $35S_{PRO}$*:NSN1-GFP* in WT genome background ($NSN1^{OX}$) from a population of ~30,000 T0 seeds. In contrast, transformation with $35S_{PRO}$*:GFP* (the control) generated 28 transgenic lines from the same size of T0 seed population under the same growth conditions. It is very likely that overexpression of *NSN1* may have deleterious effects on plant development. In situ RNA hybridization data showed that the *NSN1* mRNA transcript was

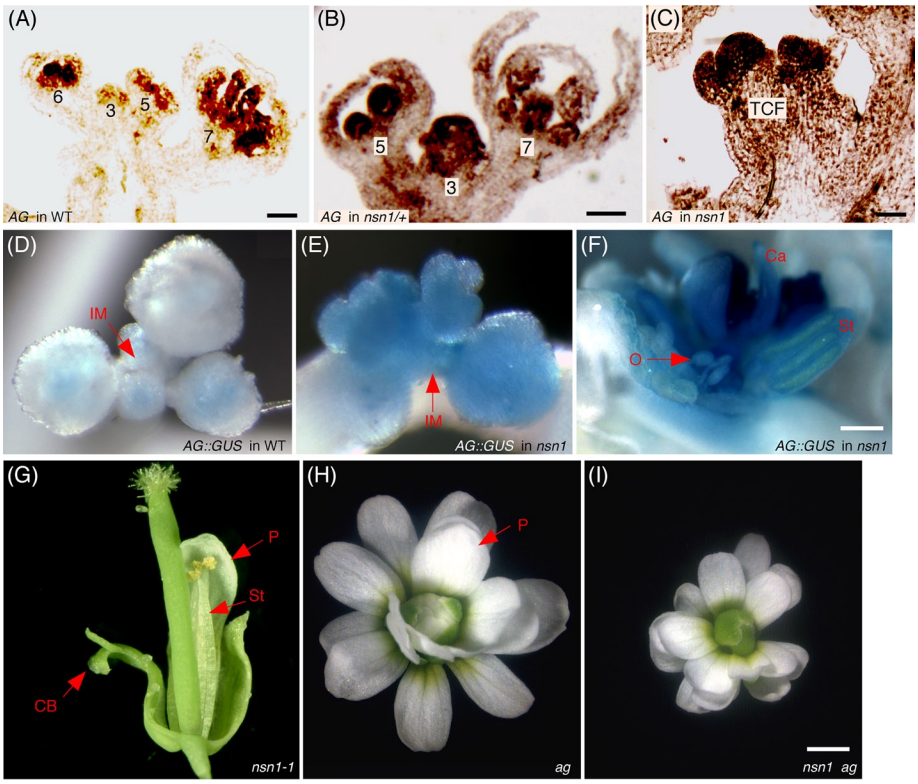

FIGURE 6: *NSN1* represses *AG* expression in inflorescence meristem and floral meristem. (A–C) In situ RNA hybridization of *AG* mRNA expression in the floral primordia of wild-type (A) and *nsn1/+* plants (B), as well as in the terminal carpelloid floral primordium of homozygous *nsn1* plant (C). (D–F) GUS staining of plants harboring KB9 in the control (D) and *nsn1* genetic background (E, F). GUS activity was elevated in the inflorescence meristem (IM) and terminal carpelloid flower of *nsn1* (F) as compared with the staining in the control plant (D). Ca, carpel-like structure; O, ectopic ovule; St, stamen-like structure. (G–I) A flower of the *nsn1 ag* double mutant (I) was morphologically identical to that of *ag* (H) but distinct from that of *nsn1-1* (G). The reduced flower size of the double mutant was a result of the difference in ecotype (*ag* in Landsberg and *nsn1* in Columbia-0). Note that the terminal carpelloid flower phenotype of *nsn1* was suppressed in the double mutant. CB, carpelloid bract; P, petal. Scale bars, 50 μm (A–F), 1 mm (G–I).

increased drastically in the SAM, flower primordia, and other tissues such as cortex and pith (Supplemental Figure S3H). Plants of $NSN1^{OX}$ were severely dwarf and bushy and lost apical dominance (Figure 8, A–C), suggesting that *NSN1* may have a role in meristem development. All branches eventually became determinate inflorescences by the development of homeotically transformed terminal flowers (Figure 8D). As compared with the terminal flowers of *nsn1*-knockout mutants (Figure 2, H and I), $NSN1^{OX}$ flowers contained sepals and petals (Figure 8, D and E) and had curled carpels (Figure 8D). Siliques of $NSN1^{OX}$ were short and curled and contained few seeds (Figure 8, F and G). Embryos were arrested at different stages of seed development (Figure 8F). We also compared the phenotypes between $NSN1^{OX}$ and *ag* mutants. Homozygous *ag* plants are known to be sterile, whereas heterozygous *ag/+* flowers have an increased number of carpels (Figure 8G). Similarly, the gynoecium of $NSN1^{OX}$ flowers often consisted of three carpels (Figure 8G). This observation is intriguing because it further supports the notion that *NSN1* may function to repress *AG* activity during floral organ development (Figure 8H).

DISCUSSION

There are three NS-related genes—*NS*, *GNL3L*, and *NGP1*—in the human and mouse genomes and only two—*AtNGP1* and *AtNSN1*—in *Arabidopsis* (Figure 1C). There have been limited studies on the biological functions of NGP1 and GNL3L, whereas the research on mammalian NS has recently attracted significant attention, partly because it is expressed specifically in adult and embryonic stem cells and in many tumors and tumor-derived cell lines (Tsai and McKay, 2002; Han *et al.*, 2005; Fan *et al.*, 2006). In this study, we present evidence showing that *Arabidopsis NSN1* is required for the maintenance of normal apical meristems and flower formation. It may act as a general negative regulator of *AG* gene expression, and this function is independent of *AP2* (Figure 8H).

NSN1 may act in a gene dosage–dependent manner and is required for flower development

Floral primordia develop from the peripheral zone of the floral meristems in plants. During floral primordia initiation, cells in the peripheral zone continue to divide and differentiate into the primordia of specialized floral organs (Lenhard *et al.*, 2001). Our in situ hybridization data (Figure 5 and Supplemental Figure S3) showed that *NSN1* mRNA is expressed in the central and peripheral zones but not in the rib zone that contributes cells to stem growth. During the development of floral primordia, *NSN1* mRNA was detectable as early as in the stage 1 primordia and was highly expressed at stages 2 to 3. After stage 3, *NSN1* expression was confined to the primordia of sepals, stamens, petals, and gyneocium.

The fact that heterozygous *nsn1/+* plants exhibited drastically defective flower phenotypes (Figure 2) implies that *NSN1* may act in a gene dosage–sensitive manner. Wild-type plants of *Arabidopsis* produce indeterminate inflorescences and only occasionally form terminal flowers under stress conditions. However, heterozygous *nsn1/+* plants produced determinate inflorescences. One to several terminal carpelloid flowers would always be found in the terminal part of inflorescences in *nsn1/+* plants (Figure 2). Homozygous *nsn1* plants exhibited severe defects in both vegetative growth and flower formation. The hypothesis of gene dosage effect of *NSN1* is also supported by evidence obtained from the overexpression of *NSN1* in a wild-type background. Transgenic plants carrying $35S_{PRO}$:*NSN1-GFP* were difficult to obtain. When they survived, they displayed an array of defects in shoot growth and flower development (Figure 8). Thus *NSN1* may act as a key regulator of flower development in *Arabidopsis*, and its function appears to depend on the gene dosage.

NSN1 controls flower organ identity by repressing *AG* gene expression

In the floral meristem, the meristematic cells sequentially produce sepal, petal, stamen, and carpel primordia. In contrast to the indeterminate shoot meristem, the floral meristem terminates at the end of flower development. The stem cells differentiate completely after

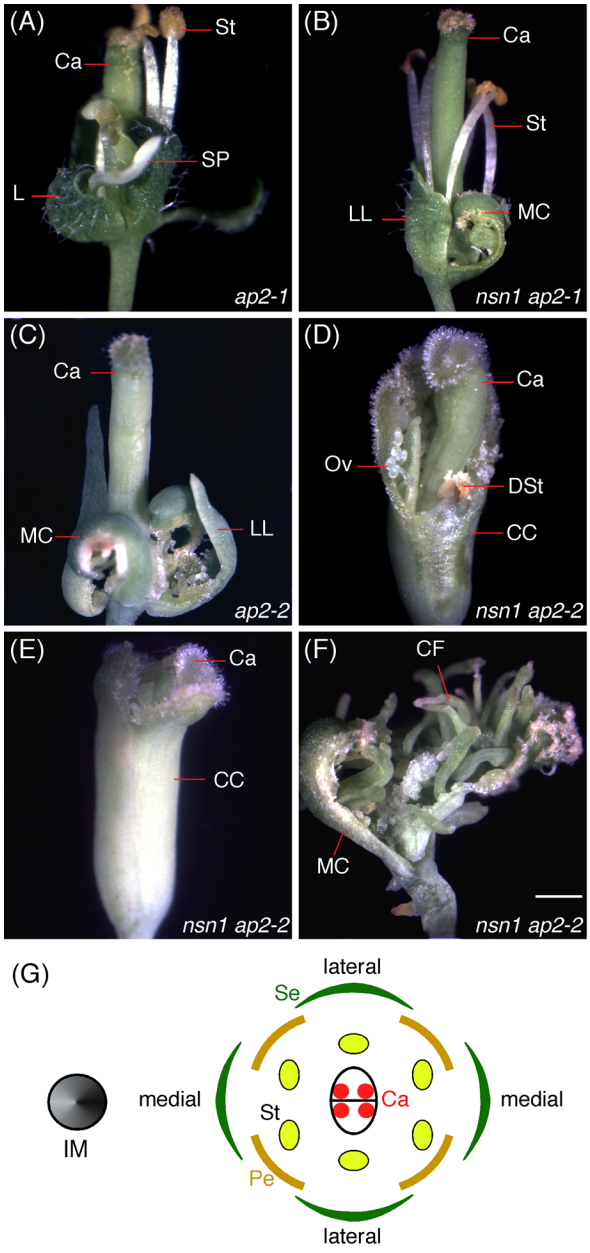

FIGURE 7: Analysis of *nsn1-1 ap2* double mutants. (A–C) Flowers of the *ap2-1* weak allele (A) and *ap2-2* severe allele (C). The *ap2-1* flower contained leafy bracts (L) in whorl 1 and staminoid petals (SP) in whorl 2, stamens (St) in whorl 3, and carpels (Ca) in whorl 4. The *ap2-2* flower had medial carpels (MC) and lateral leafy bracts (LL) in whorl 1, and no floral organs appear in whorls 2 and 3. B, Flower of *nsn1-1 ap2-1* double mutant contained medial carpels (MC) and lateral leafy bracts (LL) in whorl 1. No floral organ appears in whorl 2. (D, E) In flowers of *nsn1-1 ap2-2* double mutant, the whorl 1 organs were converted into a carpelloid cylinder (CC) that encapsulated normal whorl 4 carpels (Ca) partially (D) or completely (E). Ovules (O) and degenerated stamens (DSt) were present on the interior wall of the cylinder. (F) A terminal flower of *nsn1-1 ap2-2* contained an open gynoecium consisting of two medial carpel (MC) and numerous carpelloid filaments (CF) with stigmatic tissue on their tips. Scale bars, 1 mm (A–F). (G) Diagram of a wild-type flower with respect to the inflorescence meristem (IM). A medial position is on the same axis as IM, whereas a lateral position is on the sides of the axis. A WT flower consists of four green sepals (Se) in whorl 1, four petals (Pe) in whorl 2, six stamens (St) in whorl 3, and two fused carpels (Ca) in whorl 4. Red circles inside the carpels represent ovules.

the carpel primordia are formed. Several genes, including *AP1*, *LFY*, and *AG*, are known to play important roles during floral meristem initiation. In particular, the MADS-box transcription factor AG has a central role in the eventual termination of stem cell activity after the initiation of stamens and carpels (Yanofsky *et al.*, 1990; Mizukami and Ma, 1997; Lohmann *et al.*, 2001; Deyhle *et al.*, 2007). *AG* is not expressed in the inflorescence meristem; its expression is highly enhanced after stage 3 of floral development (Lohmann *et al.*, 2001). The relationship of *AG* and *WUS* is complicated because the activation of *AG* during floral meristem initiation requires *WUS*. It is a suicidal loop: *WUS* participates in *AG* activation in the center of the floral meristem and, in turn, the activated AG represses *WUS* expression, leading to the termination of *WUS* and stem cell activities.

In *ag* mutants, *WUS* expression persists, the stem cell activity in the floral meristem is not turned off on time, and new whorls of organs are produced indefinitely (Yanofsky *et al.*, 1990). In addition, stamens are replaced by petals and carpels are substituted by a reiteration of sepals–petals–petals in *ag* plants. *AG* expression triggers stamen and carpel development by temporally and spatially activating an array of genes involved in floral organ formation (Mizukami and Ma, 1997). Elevated *AG* expression in *blr* mutants can result in the formation of terminal carpelloid flowers and other striking floral phenotypes, including homeotic transformations from sepals to carpels (Bao *et al.*, 2004). These phenotypes coincide with the floral defects observed in *nsn1* (Figure 4). We reasoned that *NSN1* might act like BLR as a corepressor of *AG* and tested this hypothesis by assaying the GUS reporter activity in *nsn1* plants harboring the KB9 construct (*AG::GUS*). As compared with the reporter activity in the wild-type background, the GUS activity in *nsn1* was highly enhanced (Figure 6, D–F). This elevated *AG* expression level was even prominent in the terminal carpelloid flowers developed in *nsn1* plants (Figure 6F). The conclusion drawn from the *AG::GUS* reporter experiments is consistent with data obtained using *AG* mRNA in situ hybridization (Figure 6, A–C). Taken together, these data support the hypothesis that *NSN1* acts as a negative regulator of *AG* expression.

A possible role of *NSN1*

Proper regulation of *AG* transcription requires the presence of the *cis*-DNA sequences located in its 3-kb second intron, which serves as the binding site for both positive and negative regulators (Busch *et al.*, 1999; Deyholos and Sieburth, 2000; Lohmann *et al.*, 2001). *AP2* is a major negative regulator of *AG*. In fact, *AG* and *AP2* reciprocally repress one another (Bowman *et al.*, 1991; Mizukami and Ma, 1992). In addition to *AP2*, several other genes, including *LUG*, *LEUNIG_HOMOLOG* (*LUH*), *SEU*, and *BLR*, have been identified as negative regulators of *AG* gene expression (Drews *et al.*, 1991; Liu and Meyerowitz, 1995; Franks *et al.*, 2002; Bao *et al.*, 2004; Sridhar *et al.*, 2004; Sitaraman *et al.*, 2008; Das *et al.*, 2009). AP2, BLR, and PAN have been shown to bind directly to the second intron of *AG* (Deyholos and Sieburth, 2000; Bao *et al.*, 2004; Das *et al.*, 2009). In this article, we present evidence showing that *NSN1* is a new and major regulator of *AG*. It is possible that NSN1 may regulate *AG* expression via direct or indirect control of the protein complex bound to the second intro of *AG*. Because our data also suggest that *NSN1* functions in an *AP2*-independent manner (Figure 7), the regulation of *AG* by *NSN1* may occur through regulators rather than AP2 (Figure 8H). The fact that NSN1 is not a putative transcription factor but instead is a nucleolar GTP-binding protein implies the existence of a new mechanism underlying the regulation of *AG* gene expression during flower

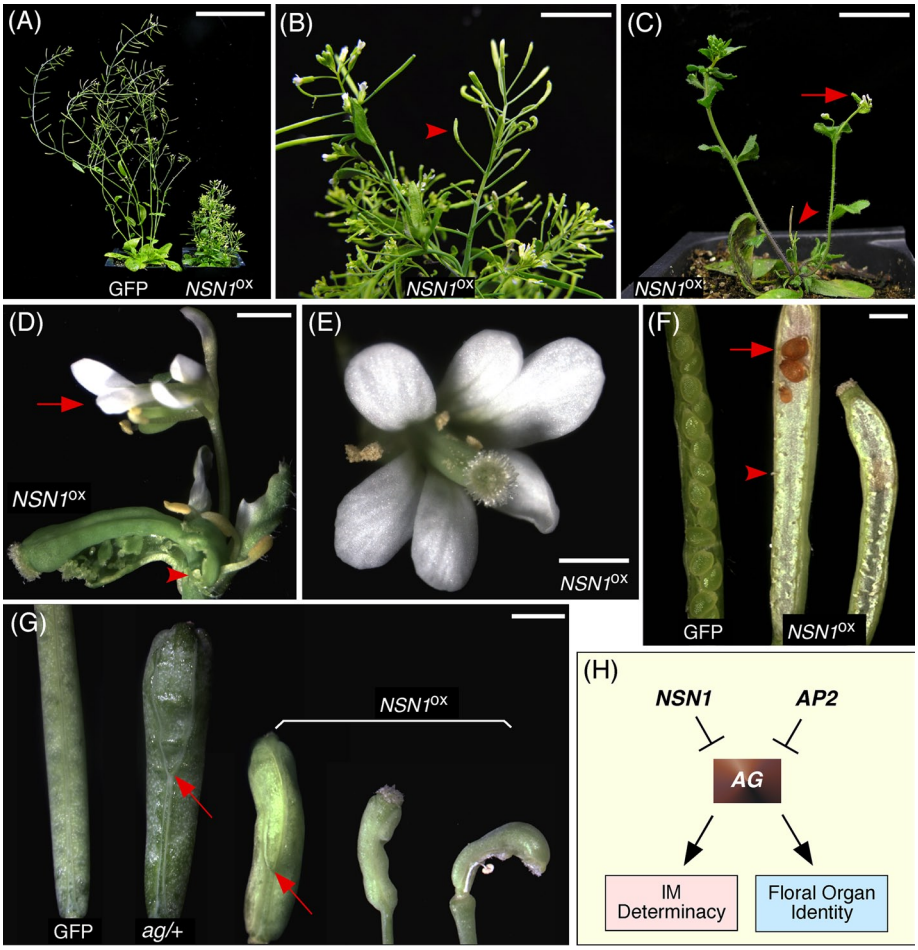

FIGURE 8: Growth and reproductive phenotypes of *NSN1*^{OX} plants. (A–D) Adult plants of *NSN1*^{OX} were dwarf and bushy (A) and produced mostly short siliques (arrowhead, B). They lost apical dominance in the main shoot (arrowhead, C) and developed a terminal flower (arrow, C) consisting of deformed sepals, petals, and stamens (arrow, D), as well as unfused carpels with ectopic ovules (arrowhead, D). (E–G) *NSN1*^{OX} plants produced flowers with an increased number of petals (E) and short and curled siliques (F) containing unfertilized ovules (arrowhead, G) and aborted embryos (arrow, G). Siliques developed from a gynoecium of three fused carpels were often seen in *NSN1*^{OX} as in *ag/+* mutant (arrows, F). Scale bars, 70 mm (A), 10 mm (B), 20 mm (C), 2 mm (D–G). (H) A proposed role of *NSN1* as a general negative regulator of *AG* in the control of inflorescence meristem (IM) determinacy and floral organ identity in *Arabidopsis*. It may exert its role in a pathway independent of *AP2*.

development. Further biochemical and genetic investigations are needed in order to understand the molecular basis of the regulation of *AG* by *NSN1*.

MATERIALS AND METHODS

Arabidopsis lines and plant growth

The *nsn1-1* T-DNA insertion line (SALK_029201) and seeds of *ap2-2* were obtained from the *Arabidopsis* Biological Resource Center (Ohio State University, Columbus, OH). The transposon insertion allele of *nsn1-2* (RAFL11-2045-1) was received from RIKEN (www.brc.riken.go.jp). Seeds of *ag/+* harboring KB9 were gifts from M. Yanofsky and D. Weigel (Busch *et al.*, 1999; Lohmann *et al.*, 2001). Plants were grown in soil under long-day conditions (16 h light/8 h darkness) at 21°C.

Genetic analysis of double mutants

To introduce KB9 into the *nsn1-1* mutant, pollen grains from the KB9 plant were crossed to the heterozygote *nsn1/+* stigma. F2 plants were analyzed for their genetic background by genomic-PCR, and heterozygote *nsn1/+* plants carrying KB9 were used for GUS staining. After GUS staining, the plant specimens were treated in 70% ethanol overnight. Images were taken under a dissection microscope (Leica, Wetzlar, Germany).

Pollen grains from *ap2-2* were used to fertilize heterozygote *nsn1/+* stigma. F1 plants were allowed for self-pollination. F2 plants were analyzed for their genetic backgrounds by genomic PCR using primers for *NSN1* and the dCAPs marker developed for *ap2-2*. F2 plants of *nsn1-1 ap2-2* double mutants were analyzed for their flower phenotypes. For generation of *nsn1-1 ag* double mutant, *ag/+* pollen grains were used to fertilize heterozygote *nsn1/+* stigma. F1 generation plants were allowed for self-pollination. F2 plants were analyzed by PCR to identify homozygote *nsn1-1 ag* double mutant. Flowers of *nsn1-1 ag* plants were photographed.

RNA isolation and RT-PCR

Total RNA was isolated from plants using RNeasy Plant Mini Kit (Qiagen, Valencia, CA). The first-strand cDNA was synthesized from 2 μg of total RNA with SuperScript First-Strand Synthesis system for RT-PCR (Invitrogen, Carlsbad, CA). A 1-μl amount of the synthesized cDNA was used for PCR amplification. Three pairs of primers were used to identity *nsn1-1* as a null mutant. One pair of primers NSN1-F and N857R1 located on the first and second exons, respectively (see Supplemental Figure S3A), were used to amplify a PCR fragment with an expected size of 133 base pairs. Nsn1-LP and Nsn1-RP located on the both sides of the T-DNA insertion were used for verification of the T-DNA. The third pair of primers, Nsn1-F and Nsn1-R, was used to determine whether the full-length *NSN1* mRNA (1760 base pairs) was present. The *ACTIN* mRNA used as an internal control was amplified using *ACTIN* primers ACT-F and ACT-R.

Peptide motif and phylogenetic analysis

Motif analysis of NSN1 was performed using ExPASy tools (www.expasy.ch/tools). For phylogenetic analysis, peptide sequences were aligned using ClustalX 2.0, and the tree was generated using Bootstrap neighboring joining program with a bootstrap value of 1000 trials. The phylogenetic tree was displayed in Phylip format on TreeView X.

Plant transformation

The coding region of *NSN1* cDNA was amplified by RT-PCR using primers NSN1-F and NSN1-R and into pCR2.1 (Invitrogen). The insert was excised with *Xho*I and *Sac*I and was subcloned into pMON-GFP. The entire cassette containing *CaMV 35S*$_{PRO}$*:NSN1-GFP:NOS3′* was excised by digestion with *Not*I and subcloned into binary vector pMON18342 (Hong *et al.*, 2001), generating

pMON-NSN1-GFP. The plasmid was introduced into *Agrobacterium tumefaciens* strain ABI by electroporation. Transformation of cultured tobacco BY-2 cells was performed as described previously (Hong *et al.*, 2001). Wild-type plants of *Arabidopsis thaliana* ecotype Columbia were transformed by the floral dip method. Transgenic BY-2 cells were selected on 1/2 MS agar plates containing 200 mg/l kanamycin and 500 mg/l carbencillin, and transgenic plants were selected on 1/2 MS agar plates containing 50 mg/l kanamycin. GFP images of the transgenic cells were taken with a Zeiss confocal laser scanning microscope (Carl Zeiss, Jena, Germany).

Complementation of *nsn1-1* mutation

A TAC clone (*JatY64G16*) containing an insert of a 77.6-kb genomic fragment in pYLTAC17 vector, obtained from the John Innes Center (Norwich, United Kingdom), was used for complementation of the *nsn1-1* mutation. The plasmid was transferred into *Agrobacterium tumefaciens* strain ABI cells by electroporation. This clone contains 19 genes, including At3g07050 (*NSN1*). Heterozygote *nsn1-1/+* plants were transformed by the *Agrobacterium*-mediated floral dip method. Transgenic plants were selected with phosphinothricin (BASTA). T2 plants that carried the transgene on the homozygote *nsn1* background were maintained. T3 plants were tested for complementation.

In situ RNA hybridization

Digoxigenin-labeled riboprobes complementary to parts of *NSN1*, *AG*, *CLAVATA 3* (*CLV3*), and *WUS* genes were used to detect their mRNAs in inflorescence and floral meristems as described (Goodrich *et al.*, 1997). The *NSN1* cDNA fragment corresponding to the C-terminal half of its coding region was amplified by PCR using primers NSN1-LP and NSN1-RP and cloned into pCRII (Invitrogen) to yield pNSN. The plasmid was linearized with *Apa*I and transcribed with SP6 RNA polymerase (Roche, Indianapolis, IN) to produce antisense RNA probe. For the control with the *NSN1* sense RNA probe, pNSN1 was linearized with *Bam*H1 and transcribed with T7 RNA polymerase (Roche). For *AGAMOUS* probe, cDNA fragment was amplified by *AG* primers AG-F and AG-R as described previously (Yanofsky *et al.*, 1990).

Histology and GUS staining

Plant tissues were fixed in FAA solution (3.7% formaldehyde, 5% acetic acid, and 50% ethanol) at room temperature for 16 h. The fixed tissues were dehydrated in a series of ethanol (30, 50, 70, 85, 90, and 100%), cleared with xylene, and embedded in Paraplast (Sigma-Aldrich, St. Louis, MO) as described previously (Causier *et al.*, 2005). Serial 8-μm-thick sections were transferred to polylysine-coated slides (Sigma-Aldrich) and stained with 0.01% toludine blue for 5–10 min at room temperature after dewaxing. GUS staining was performed as described (Schoof *et al.*, 2000).

Scanning electronic microscopy

Plant tissues were fixed overnight in 50 mM phosphate butter containing 2% glutaraldehyde and 2% paraformaldehyde. Fixed tissues were rinsed three times with 50 mM phosphate buffer and kept in osmium tetroxide (1%) overnight at 4°C. The tissues were rinsed three times with 50 mM phosphate buffer and dehydrated in a 30, 50, 70, 95, and 100% alcohol gradient. After critical point drying, the tissues were coated with gold and observed under scanning electronic microscopy.

ACKNOWLEDGMENTS

We thank A. Caplan for critical comments on the manuscript and the *Arabidopsis* Biological Resource Center, RIKEN, and M. Yanofsky, T. Laux, and D. Weigel for providing *Arabidopsis* seeds. We also thank Haiqing Sheng, Shizhen Gu, and Christina Mitchell for technical assistance during the course of this study. This work was supported by National Science Foundation grants (MCB 0548525 and IOB 0543923 to Z.H.) and an IDeA Network of Biomedical Research Excellence Scholars Program (National Institutes of Health/National Center for Research Resources P20RR016454) Fellowship (to D.K.G.).

REFERENCES

Bao X, Franks RG, Levin JZ, Liu Z (2004). Repression of *AGAMOUS* by *BELLRINGER* in floral and inflorescence meristems. Plant Cell 16, 1478–1489.

Beekman C, Nichane M, De Clercq S, Maetens M, Floss T, Wurst W, Bellefroid E, Marine JC (2006). Evolutionarily conserved role of nucleostemin: controlling proliferation of stem progenitor cells during early vertebrate development. Mol Cell Biol 26, 9291–9301.

Bowman JL, Smyth DR, Meyerowitz EM (1989). Genes directing flower development in *Arabidopsis*. Plant Cell 1, 37–52.

Bowman JL, Smyth DR, Meyerowitz EM (1991). Genetic interactions among floral homeotic genes of *Arabidopsis*. Development 112, 1–20.

Busch MA, Bomblies K, Weigel D (1999). Activation of a floral homeotic gene in *Arabidopsis*. Science 285, 585–587.

Causier B, Castillo R, Zhou J, Ingram R, Xue Y, Schwarz-Sommer Z, Davies B (2005). Evolution in action: following function in duplicated floral homeotic genes. Curr Biol 15, 1508–1512.

Chen X, Liu J, Cheng Y, Jia D (2002). *HEN1* functions pleiotropically in *Arabidopsis* development and acts in C function in the flower. Development 129, 1085–1094.

Chen X, Meyerowitz EM (1999). *HUA1* and *HUA2* are two members of the floral homeotic *AGAMOUS* pathway. Mol Cell 3, 349–360.

Dai MS, Sun XX, Lu H (2008). Aberrant expression of nucleostemin activates p53 and induces cell cycle arrest via inhibition of MDM2. Mol Cell Biol 28, 4365–4376.

Daigle DM, Rossi L, Berghuis AM, Aravind L, Koonin EV, Brown ED (2002). YjeQ, an essential, conserved, uncharacterized protein from *Escherichia coli*, is an unusual GTPase with circularly permuted G-motifs and marked burst kinetics. Biochemistry 41, 11109–11117.

Das P, Ito T, Wellmer F, Vernoux T, Dedieu A, Traas J, Meyerowitz EM (2009). Floral stem cell termination involves the direct regulation of *AGAMOUS* by *PERIANTHIA*. Development 136, 1605–1611.

Deyhle F, Sarkar AK, Tucker J, Laux T (2007). *WUSCHEL* regulates cell differentiation during anther development. Dev Biol 302, 154–159.

Deyholos MK, Sieburth LE (2000). Separable whorl-specific expression and negative regulation by enhancer elements within the *AGAMOUS* second intron. Plant Cell 12, 1799–1810.

Drews GN, Bowman JL, Meyerowitz EM (1991). Negative regulation of the *Arabidopsis* homeotic gene *AGAMOUS* by the *APETALA2* product. Cell 65, 991–1002.

Du X, Rao MR, Chen XQ, Wu W, Mahalingam S, Balasundaram D (2006). The homologous putative GTPases Grn1p from fission yeast and the human GNL3L are required for growth and play a role in processing of nucleolar pre-rRNA. Mol Biol Cell 17, 460–474.

Fan Y, Liu Z, Zhao S, Lou F, Nilsson S, Ekman P, Xu D, Fang X (2006). Nucleostemin mRNA is expressed in both normal and malignant renal tissues. Br J Cancer 94, 1658–1662.

Franks RG, Wang C, Levin JZ, Liu Z (2002). *SEUSS*, a member of a novel family of plant regulatory proteins, represses floral homeotic gene expression with *LEUNIG*. Development 129, 253–263.

Goodrich J, Puangsomlee P, Martin M, Long D, Meyerowitz EM, Coupland G (1997). A Polycomb-group gene regulates homeotic gene expression in *Arabidopsis*. Nature 386, 44–51.

Han C, Zhang X, Xu W, Wang W, Qian H, Chen Y (2005). Cloning of the nucleostemin gene and its function in transforming human embryonic bone marrow mesenchymal stem cells into F6 tumor cells. Int J Mol Med 16, 205–213.

Hong Z, Delauney AJ, Verma DP (2001). A cell plate-specific callose synthase and its interaction with phragmoplastin. Plant Cell 13, 755–768.

Jafarnejad SM, Mowla SJ, Matin MM (2008). Knocking-down the expression of nucleostemin significantly decreases rate of proliferation of rat bone

marrow stromal stem cells in an apparently p53-independent manner. Cell Prolif 41, 28–35.
Jofuku KD, den Boer BG, Van Montagu M, Okamuro JK (1994). Control of *Arabidopsis* flower and seed development by the homeotic gene *APETALA2*. Plant Cell 6, 1211–1225.
Kudron MM, Reinke V (2008). *C. elegans* nucleostemin is required for larval growth and germline stem cell division. PLoS Genet 4, e1000181.
Lenhard M, Bohnert A, Jurgens G, Laux T (2001). Termination of stem cell maintenance in *Arabidopsis* floral meristems by interactions between *WUSCHEL* and *AGAMOUS*. Cell 105, 805–814.
Liu Z, Meyerowitz EM (1995). *LEUNIG* regulates *AGAMOUS* expression in *Arabidopsis* flowers. Development 121, 975–991.
Lohmann JU, Hong RL, Hobe M, Busch MA, Parcy F, Simon R, Weigel D (2001). A molecular link between stem cell regulation and floral patterning in *Arabidopsis*. Cell 105, 793–803.
Ma H, Pederson T (2007). Depletion of the nucleolar protein nucleostemin causes G1 cell cycle arrest via the p53 pathway. Mol Biol Cell 18, 2630–2635.
Meng L, Zhu Q, Tsai RY (2007). Nucleolar trafficking of nucleostemin family proteins: common versus protein-specific mechanisms. Mol Cell Biol 27, 8670–8682.
Mizukami Y, Ma H (1992). Ectopic expression of the floral homeotic gene *AGAMOUS* in transgenic *Arabidopsis* plants alters floral organ identity. Cell 71, 119–131.
Mizukami Y, Ma H (1997). Determination of *Arabidopsis* floral meristem identity by *AGAMOUS*. Plant Cell 9, 393–408.
Politz JC, Polena I, Trask I, Bazett-Jones DP, Pederson T (2005). A nonribosomal landscape in the nucleolus revealed by the stem cell protein nucleostemin. Mol Biol Cell 16, 3401–3410.
Reynaud EG, Andrade MA, Bonneau F, Ly TB, Knop M, Scheffzek K, Pepperkok R (2005). Human Lsg1 defines a family of essential GTPases that correlates with the evolution of compartmentalization. BMC Biol 3, 21.
Romanova L, Grand A, Zhang L, Rayner S, Katoku-Kikyo N, Kellner S, Kikyo N (2009). Critical role of nucleostemin in pre-rRNA processing. J Biol Chem 284, 4968–4977.
Schoof H, Lenhard M, Haecker A, Mayer KF, Jurgens G, Laux T (2000). The stem cell population of *Arabidopsis* shoot meristems is maintained by a regulatory loop between the *CLAVATA* and *WUSCHEL* genes. Cell 100, 635–644.
Sieburth LE, Meyerowitz EM (1997). Molecular dissection of the *AGAMOUS* control region shows that *cis* elements for spatial regulation are located intragenically. Plant Cell 9, 355–365.
Sieburth LE, Running MP, Meyerowitz EM (1995). Genetic separation of third and fourth whorl functions of *AGAMOUS*. Plant Cell 7, 1249–1258.
Sitaraman J, Bui M, Liu Z (2008). *LEUNIG HOMOLOG* and *LEUNIG* perform partially redundant functions during *Arabidopsis* embryo and floral development. Plant Physiol 147, 672–681.
Sridhar VV, Surendrarao A, Gonzalez D, Conlan RS, Liu Z (2004). Transcriptional repression of target genes by LEUNIG and SEUSS, two interacting regulatory proteins for *Arabidopsis* flower development. Proc Natl Acad Sci USA 101, 11494–11499.
Sun B, Xu Y, Ng KH, Ito T (2009). A timing mechanism for stem cell maintenance and differentiation in the *Arabidopsis* floral meristem. Genes Dev 23, 1791–1804.
Tsai RY, McKay RD (2002). A nucleolar mechanism controlling cell proliferation in stem cells and cancer cells. Genes Dev 16, 2991–3003.
Tsai RY, McKay RD (2005). A multistep, GTP-driven mechanism controlling the dynamic cycling of nucleostemin. J Cell Biol 168, 179–184.
Yanofsky MF, Ma H, Bowman JL, Drews GN, Feldmann KA, Meyerowitz EM (1990). The protein encoded by the *Arabidopsis* homeotic gene *AGAMOUS* resembles transcription factors. Nature 346, 35–39.
Zhu Q, Yasumoto H, Tsai RY (2006). Nucleostemin delays cellular senescence and negatively regulates TRF1 protein stability. Mol Cell Biol 26, 9279–9290.